A Modified Single-Phase Quasi-Z-Source AC–AC Converter

Minh-Khai Nguyen, *Student Member, IEEE*, Young-Cheol Lim, *Member, IEEE*, and Yong-Jae Kim, *Member, IEEE*

***Abstract*—A modified single-phase quasi-Z-source ac–ac converter is proposed in this paper. The proposed converter has the main features in that the output voltage can be bucked or boosted and be both in-phase and out-of-phase with the input voltage. The input voltage and output voltage share the same ground, the size of a converter is reduced, and it operates in a continuous current mode. A safe-commutation strategy for the modified single-phase quasi-Z-source ac–ac converter is used instead of a snubber circuit. The operating principles and a steady-state analysis are presented. A laboratory prototype, tested using a resistive load, a passive load, and a nonlinear load, was constructed that used an input voltage of 70 V_{rms}/60 Hz in order to verify the performance of the modified single-phase quasi-Z-source ac–ac converter. The experimental results verified that the converter has a lower input current total harmonic distortion, a higher input power factor, and a higher efficiency in comparison to a conventional single-phase Z-source ac–ac converter. In addition, the experimental results show that the use of the safe-commutation strategy is a significant improvement, as it makes it possible to avoid voltage spikes on the switches.**

***Index Terms*—Buck–boost capability, pulsewidth modulation (PWM), quasi-Z-source converter, reversing and maintaining phase angle, safe-commutation, single-phase ac–ac converter, total harmonic distortion (THD).**

I. Introduction

In industrial practice, ac–ac line conditioners or ac–ac conversions are commonly implemented using ac thyristor power controllers, which employ the phase angle or integral cycle control on the ac supply in order to obtain a desired output voltage. However, they have some significant disadvantages, such as a low input power factor, a high total harmonic distortion (THD) in the source current, and a poor power transfer efficiency. Often ac controllers can be replaced by pulsewidth modulation (PWM) ac chopper controllers, which have the following features: provisions for a better power factor, transient response and efficiency, a low harmonic current in the line, and smaller input–output filter parameters [1]–[5]. AC–AC converters can perform conditioning, isolating, and input power filtering in addition to voltage regulation. Direct PWM ac–ac converters can be derived from dc–dc topologies; all of the unidirectional switches are substituted with bidirectional devices [5].

A class of single-phase PWM ac–ac power converters with simple topologies have been presented in [4]–[10]. These include buck, boost, buck–boost, and Cuk converters. However, each topology has its drawbacks. An increase of the output voltage above the input voltage is not possible using the buck topology found in [4]–[6]. A decrease of the output voltage under the input voltage is not possible for the boost topology found in [4] and [5]. The buck–boost and Cuk topologies found in [4] and [5] enable the output voltage to be either lower or higher than the input voltage with a reversible phase angle. However, there are discontinuous input and output currents found in the former case. The multilevel or multicell ac–ac converters found in [7]–[9] are step-down multilevel circuits based on the concept of flying capacitors that reduce the voltage stress on the switches and improve the quality of the output voltage. In the multicell converters, however, the voltage of the flying capacitors needs to be in a constant proportion to the input voltage. Therefore, a balancing circuit, such as an *RLC* booster, needs to be connected in parallel to the converter load in order to reduce the imbalance [7], [8]. For isolated ac–ac topologies, current-mode ac–ac converters with high-frequency ac links using a two-stage power conversion were presented in [10]. Direct PWM ac–ac converters can be used to overcome voltage sags and swells [11]–[13] or to compensate for a static VAr [14] in power systems. It has also been reported that the use of safe-commutation switches with the PWM control can significantly improve an ac–ac converter performance [15]–[18].

Z-source converters applied to dc–ac inverters and ac–ac converters have recently been proposed in [1]–[3], [15], [16], and [19]–[31]. The research on Z-source dc–ac inverters has been focused on the PWM strategy, modeling and control [19], [20], applications [21], high boost factors [22], [23], and other Z-network topologies [24]–[30]. The research on Z-source ac–ac converters has been focused on single-phase topologies [1]–[3], [15], [16] and three-phase topologies [31]. A family of quasi-Z-source converters has been presented in [3], [24], and [25] that overcome the inconveniences found in traditional Z-source inverters. Quasi-Z-source converters have advantages, such as reducing the passive component ratings and improving the input profiles.

Manuscript received January 3, 2011; revised March 8, 2011, and May 12, 2011; accepted May 12, 2011. Date of current version December 16, 2011. This work was supported in part by the grant from the Korean Ministry of Education, Science and Technology (The Regional Core Research Program/Biohousing Research Institute), and in part by the Human Resources Development of the Korea Institute of Energy Technology Evaluation and Planning funded by the Korea Government Ministry of Knowledge Economy under Grant 2007-P-EP-HM-E-09-0000. Recommended for publication by Associate Editor J. A. Pomilio.

M.-K. Nguyen is with the Department of Electrical and Electronic Engineering, Nguyen Tat Thanh University, Ho Chi Minh City 70000, Vietnam (e-mail: khaibk@ieee.org).

Y.-C. Lim is with the Department of Electrical Engineering, Chonnam National University, Buk-gu, Gwangju 500-757, Korea (e-mail: yclim@chonnam.ac.kr).

Y.-J. Kim is with the Department of Electrical Engineering, Chosun University, Dong-gu, Gwangju 501-759, Korea (e-mail: kimyj21@chosun.ac.kr).

Digital Object Identifier 10.1109/TPEL.2011.2157362

The conventional single-phase Z-source PWM ac–ac converters proposed in [1] and [2] have main features in that the output voltage can be bucked/boosted and be in-phase/out-of-phase with the input voltage. However, the conventional Z-source PWM ac–ac converters found in [1] and [2] have a significant drawback in that the input current is operated in a discontinuous current mode. When the input current operates in this discontinuous current mode, its waveform is nonsinusoidal, which increases the input current THD. Moreover, the peak of the input current in the discontinuous current mode is higher than it is in the continuous current mode. Another drawback is that the input voltage and the output voltage of the original Z-source PWM ac–ac converter [1] do not share the same ground. As a result, the desired feature that enables the output voltage to reverse or maintain its phase angle relative to the input voltage is not well supported. In an effort to overcome the inconveniences of the traditional Z-source ac–ac converters, a single-phase quasi-Z-source ac–ac converter has recently been proposed in [3]. In comparison to the conventional Z-source ac–ac converters, the single-phase quasi-Z-source ac–ac converter has the following unique advantages: the input voltage and the output voltage share the same ground; the converter operates in the continuous current mode with special features such as a reduction in the in-rush, a harmonic current, an improved power factor, and an efficient power transfer.

In this paper, a modified single-phase quasi-Z-source ac–ac converter without input or output filters is presented. The proposed converter inherits all of the advantages of the traditional single-phase Z-source ac–ac converter; it has buck–boost capabilities and can maintain or reverse the output phase angle all the while sharing the same ground. Moreover, the modified single-phase quasi-Z-source ac–ac converter has the following unique advantages: a smaller converter size, an operation in the continuous current mode that enables special features such as a reduction in the in-rush, a harmonic current, an improved power factor, and an increased efficiency. A safe-commutation strategy is provided for the proposed converter that eliminates voltage spikes on the switches without the need for a snubber circuit. The operating principles, compared to those of a conventional single-phase Z-source ac–ac converter, are thoroughly outlined.

In order to verify the proposed converter, a laboratory prototype based on a TMS320F2812 digital signal processor (DSP) was built and connected to a resistive load R, a passive load RL, and a nonlinear load. The experimental results show that the output voltage can be boosted and be in-phase with the input voltage, as well as bucked/boosted and be out-of-phase with the input voltage. The experimental results show that the use of the safe-commutation strategy provides a significant improvement, in that it avoids voltage spikes on the switches. Moreover, in order to fully explore the merits of the modified single-phase quasi-Z-source ac–ac converter, when compared to other conventional single-phase Z-source ac–ac converters, the experimental results exhibit a lower input-current THD, a higher input power factor, and a higher efficiency. The proposed converter effectively becomes a "solid-state transformer" with a continuously variable turn ratio. The proposed converter can be used as a dynamic voltage restorer to compensate for voltage sags and swells in ac–ac line conditioning without requiring large energy-storage devices.

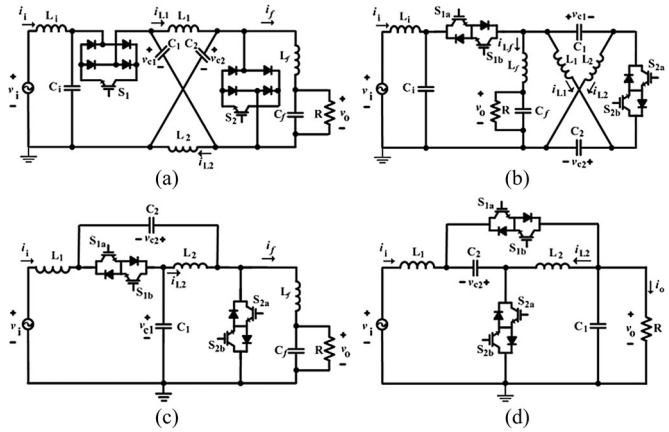

Fig. 1. Single-phase Z-source ac–ac converter topologies. (a) Original single-phase Z-source ac–ac converter with *LC* input/output filter with no ground sharing [1]. (b) Conventional single-phase Z-source ac–ac converter with *LC* input/output filters and ground sharing [2]. (c) Single-phase quasi-Z-source ac–ac converter with ground sharing, an, *LC* output filter, and no *LC* input filter [3]. (d) Modified single-phase quasi-Z-source ac–ac converter with ground sharing and no *LC* input/output filters.

II. Modified Single-Phase Quasi-Z-Source AC–AC Converter

Fig. 1 shows the single-phase Z-source ac–ac converters discussed in this paper. The original single-phase Z-source ac–ac converter [1] with an *LC* input/output filter and no shared ground is shown in Fig. 1(a). Fig. 1(b) shows the conventional single-phase Z-source ac–ac converter [2] with an *LC* input/output filter and a shared ground. In Fig. 1(c), a single-phase quasi-Z-source ac–ac converter [3] with a shared ground and an *LC* output filter but no *LC* input filter is presented. The proposed modified single-phase quasi-Z-source ac–ac converter with a shared ground and no *LC* input/output filters is shown in Fig. 1(d). In the conventional converters [1], [2], as shown in Fig. 1(a) and 1(b), an *LC* input filter is required in order to reduce the switching ripple found in the input current. Furthermore, in the original converter [1], as shown in Fig. 1(a), a small snubber circuit is added for each switch in order to limit the voltage overshoot and to provide commutation paths during the dead times; this results in inefficiency and unreliability. In the single-phase quasi-Z-source ac–ac converter [3], as shown in Fig. 1(c), an *LC* input filter cannot be added because inductor L_1 connects directly to the input. However, an *LC* output filter needs to be added in order to decrease the high harmonic components that appear on the load side. In a compact topology, the modified single-phase Z-source ac–ac converter, as shown in Fig. 1(d), uses only a quasi-Z-source network with two inductors L_1, L_2, two capacitors C_1, C_2, and two bidirectional switches S_{1j}, S_{2j} ($j = a, b$). Because the load is directly connected to capacitor C_1, the *LC* output filter can be omitted. Therefore, the modified single-phase Z-source ac–ac converter topology is smaller when compared to the other topologies.

A. Commutation Problem

The two bidirectional switches, S_{1j} and S_{2j} ($j = a, b$), are able to block voltage and conduct current in both directions. Because true bidirectional switches are not available to date, they can be implemented by the connection of two diodes and two insulated gate bipolar transistors (IGBTs) in an anti-parallel (common emitter back to back) manner, as shown in Fig. 1(d) [14], [15]. The single-phase quasi-Z-source ac–ac converters shown in Fig. 1(c) and (d) have a commutation problem. A change in the current due to the PWM switching will result in current and voltage spikes. Note that the current spikes are generated by the short-circuit or shoot-through path; the voltage spikes are produced because of the current derivative of the inductance. Both types of spikes will destroy the switches due to stress [14], [15]. In order to understand the commutation problem found in single-phase quasi-Z-source ac–ac converters, take the circuit shown in Fig. 1(d) as an example. Suppose that S_{1j} ($j = a, b$) is turned ON and conducts current. After a time, we want to commutate the current to S_{2j} ($j = a, b$). Theoretically, the switching must be instantaneous and simultaneous. For practical reasons, however, we have to take into account the finite switching times and delays found in the drive circuits and switches. Therefore, if S_{2j} ($j = a, b$) is turned ON before S_{1j} ($j = a, b$) is turned OFF, a short-circuit path is established through S_{1j}–C_1–S_{2j}–C_2 causing current spikes that will destroy the devices. Similarly, if S_{1j} ($j = a, b$) is turned OFF before S_{2j} ($j = a, b$) is turned ON, there will be a junction that connects inductors L_1 and L_2 resulting in voltage spikes that will destroy the switches. In some previous methods, a lossy snubber circuit is added for each switch in order to limit the voltage overshoot. This provides commutation paths in the dead times that results in inefficiency and unreliability.

The modified single-phase quasi-Z-source ac–ac converter does not require a snubber circuit because a safe-commutation strategy is used. The safe-commutation scheme establishes a continuous current path in the dead times that eliminates voltage spikes on the switches. Therefore, the modified single-phase quasi-Z-source ac–ac converter has a smaller size and a higher efficiency in comparison to the conventional converters presented in [1]–[3].

B. Operating Principles

Fig. 2 illustrates the switching strategy of the modified single-phase quasi-Z-source ac–ac converter. In the in-phase mode where the input voltage and the output voltage are in the same phase, if the input voltage $v_i > 0$, switches S_{1a} and S_{2b} are fully turned ON while S_{1b} and S_{2a} are modulated complementary to the dead time. If $v_i < 0$, switches S_{1b} and S_{2a} are fully turned ON while S_{1a} and S_{2b} are modulated complementary to the dead time. In the out-of-phase mode in which the input voltage and the output voltage are in opposite phases, if $v_i > 0$, switches S_{1b} and S_{2a} are fully turned ON while S_{1a} and S_{2b} are modulated complementary to the dead time. If $v_i < 0$, switches S_{1a} and S_{2b} are fully turned ON while S_{1b} and S_{2a} are modulated complementary to the dead time. As indicated in Fig. 2, D refers to the equivalent duty ratio and T is the switching period.

Fig. 3 shows the operation states in the in-phase mode when $v_i > 0$. Switches S_{1a} and S_{2b} are fully turned ON while S_{1b} and S_{2a} are modulated complementary to the dead time. In state 1, as shown in Fig. 3(a), S_{1a} is turned ON and conducts the current during the increasingly positive cycle of the input voltage; S_{1b} is turned ON and conducts the negative current from the load to the source, if possible; S_{2b} is turned ON for commutation purposes. S_{1b} is then turned OFF while S_{2a} has not yet turned ON, and so there are two commutation states that occur. If $i_i + i_{L2} > 0$, the current flows along a path from S_{1a}, as shown in Fig. 3(b); if $i_i + i_{L2} < 0$, the current flows along a path from S_{2b}, as shown in Fig. 3(c). In state 2, as shown in Fig. 3(d), S_{2a} is turned ON and conducts the current from the source to the load; S_{2b} is turned ON and conducts the negative current from the load to the source, if possible; S_{1a} is turned ON for commutation purposes. In these switching patterns, the current path is always continuous regardless of the current direction. This eliminates the voltage spikes during the switching and commutation processes. The analysis when $v_i < 0$ is similar to that found when $v_i > 0$. The dotted line

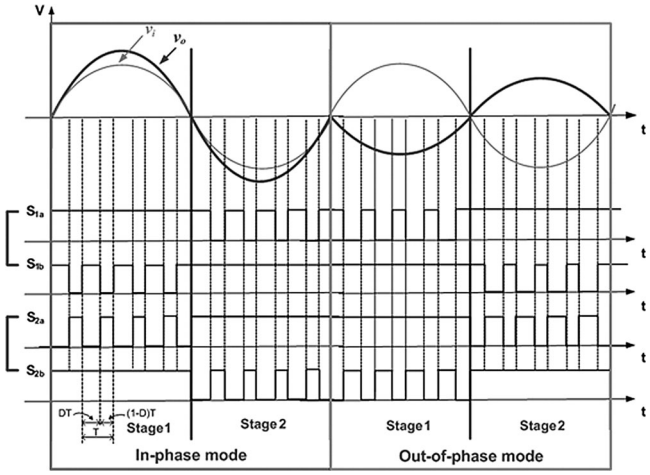

Fig. 2. Switching pattern of the modified single-phase quasi-Z-source ac–ac converter (D is the duty ratio; T is the switching period).

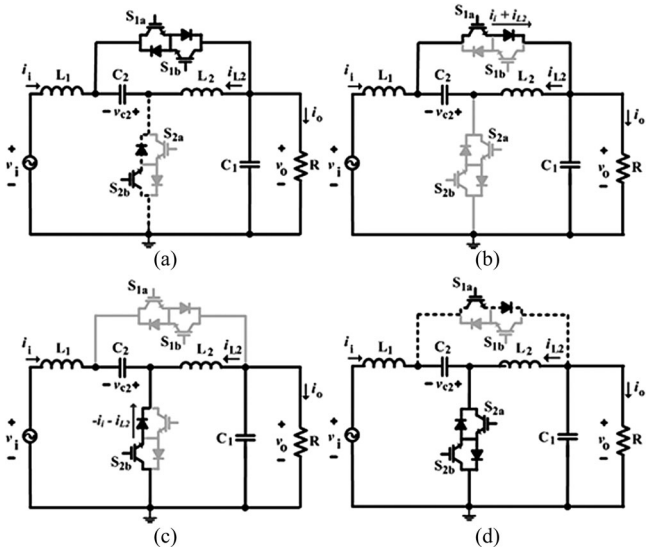

Fig. 3. Operation states of the modified single-phase quasi-Z-source ac–ac converter in the in-phase mode when $v_i > 0$. (a) State 1. (b)Commutation state when $i_i + i_{L2} > 0$. (c) Commutation state when $i_i + i_{L2} < 0$. (d) State 2.

TABLE I
SWITCHING CONTROL SEQUENCE FOR THE MODIFIED SINGLE-PHASE QUASI-Z-SOURCE AC–AC CONVERTER OPERATION

Mode	v_i	Switch "on" states			
		State 1		State 2	
		Active	Commutation	Active	Commutation
In-phase	>0	S_{1a}, S_{1b}	S_{2b}	S_{2a}, S_{2b}	S_{1a}
	<0	S_{1a}, S_{1b}	S_{2a}	S_{2a}, S_{2b}	S_{1b}
Out-of-phase	>0	S_{1a}, S_{1b}	S_{2a}	S_{2a}, S_{2b}	S_{1b}
	<0	S_{1a}, S_{1b}	S_{2b}	S_{2a}, S_{2b}	S_{1a}

in Fig. 3 indicates the safe-commutation switch during each particular stage. Table I provides the switching sequences for the operations of the modified single-phase quasi-Z-source ac–ac converter.

C. Circuit Analysis

A circuit analysis of the modified single-phase quasi-Z-source ac–ac converter begins with the following assumptions: 1) the converter is operating in the continuous conduction mode; 2) the parasitic resistances of L_1 and L_2 are the same and equal and denoted by r_L; 3) the equivalent series resistances of C_1 and C_2 are the same and equal and denoted by r_C; 4) the on-resistance of the switches S_{1j} and S_{2j} ($j = a, b$) are the same and equal and denoted by r_s; and 5) the switching frequency is more than the frequency of the input and output voltages.

Ignoring the dead time effects, the modified single-phase quasi-Z-source ac–ac converter has two operating states in one switching period, which are denoted as state 1 and state 2, as shown in Fig. 4(a) and (b), respectively. In state 1, S_{1j} is turned ON and S_{2j} is turned OFF, as shown in Fig. 4(a). The time interval of this state is DT, where D is the equivalent duty ratio of S_{1j} and T is the switching period, as shown in Fig. 2. Therefore

$$\begin{bmatrix} L_1 & 0 & 0 & 0 \\ 0 & L_2 & 0 & 0 \\ 0 & 0 & C_1 & 0 \\ 0 & 0 & 0 & C_2 \end{bmatrix} \frac{d}{dt} \begin{bmatrix} i_i(t) \\ i_{L2}(t) \\ v_o(t) \\ v_{C2}(t) \end{bmatrix} = \begin{bmatrix} -(r_L + r_s) & -r_s & -1 & 0 \\ -r_s & -(r_L + r_C + r_s) & 0 & -1 \\ 1 & 0 & -1/R & 0 \\ 0 & 1 & 0 & 0 \end{bmatrix} \times \begin{bmatrix} i_i(t) \\ i_{L2}(t) \\ v_o(t) \\ v_{C2}(t) \end{bmatrix} + \begin{bmatrix} v_i(t) \\ 0 \\ 0 \\ 0 \end{bmatrix}. \quad (1)$$

In state 2, S_{1j} is turned OFF and S_{2j} is turned ON, as shown in Fig. 4(b). The time interval of this state is $(1-D)T$. Therefore

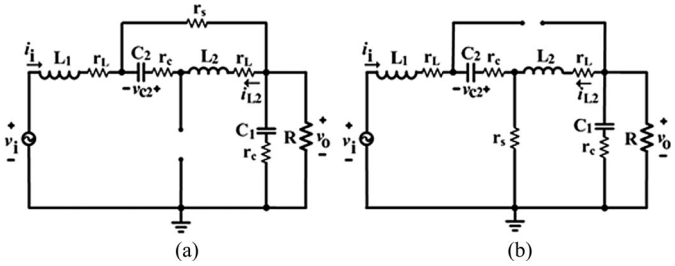

Fig. 4. Equivalent circuits for the proposed converter. (a) State 1. (b) State 2.

$$\begin{bmatrix} L_1 & 0 & 0 & 0 \\ 0 & L_2 & 0 & 0 \\ 0 & 0 & C_1 & 0 \\ 0 & 0 & 0 & C_2 \end{bmatrix} \frac{d}{dt} \begin{bmatrix} i_i(t) \\ i_{L2}(t) \\ v_o(t) \\ v_{C2}(t) \end{bmatrix} = \begin{bmatrix} -(r_L + r_C + r_s) & -r_s & 0 & 1 \\ -r_s & -(r_L + r_s) & 1 & 0 \\ 0 & -1 & -1/R & 0 \\ -1 & 0 & 0 & 0 \end{bmatrix} \times \begin{bmatrix} i_i(t) \\ i_{L2}(t) \\ v_o(t) \\ v_{C2}(t) \end{bmatrix} + \begin{bmatrix} v_i(t) \\ 0 \\ 0 \\ 0 \end{bmatrix}. \quad (2)$$

From (1) and (2), the following averaged equation is obtained

$$\begin{bmatrix} L_1 & 0 & 0 & 0 \\ 0 & L_2 & 0 & 0 \\ 0 & 0 & C_1 & 0 \\ 0 & 0 & 0 & C_2 \end{bmatrix} \frac{d}{dt} \begin{bmatrix} i_i(t) \\ i_{L2}(t) \\ v_o(t) \\ v_{C2}(t) \end{bmatrix} = \begin{bmatrix} -(r_L + r_s) - (1-D)r_C & -r_s & -D & 1-D \\ -r_s & -(r_L + r_s) - Dr_C & 1-D & -D \\ D & -(1-D) & -1/R & 0 \\ -(1-D) & D & 0 & 0 \end{bmatrix} \times \begin{bmatrix} i_i(t) \\ i_{L2}(t) \\ v_o(t) \\ v_{C2}(t) \end{bmatrix} + \begin{bmatrix} v_i(t) \\ 0 \\ 0 \\ 0 \end{bmatrix}. \quad (3)$$

In the steady state, it is found that

$$\begin{bmatrix} L_1 & 0 & 0 & 0 \\ 0 & L_2 & 0 & 0 \\ 0 & 0 & C_1 & 0 \\ 0 & 0 & 0 & C_2 \end{bmatrix} \frac{d}{dt} \begin{bmatrix} i_i(t) \\ i_{L2}(t) \\ v_o(t) \\ v_{C2}(t) \end{bmatrix} = \begin{bmatrix} 0 \\ 0 \\ 0 \\ 0 \end{bmatrix}. \quad (4)$$

Thus

$$\begin{cases} v_o = \dfrac{D(2D-1)R}{(2D-1)^2R + r_s + (2D^2-2D+1)r_L + D(1-D)r_C} v_i \\ v_{c2} = \dfrac{(1-D)(2D-1)R - r_s - (1-D)r_L - D(1-D)r_C}{(2D-1)^2R + r_s + (2D^2-2D+1)r_L + D(1-D)r_C} v_i \\ i_i = \dfrac{D}{2D-1}\dfrac{v_o}{R} \\ i_{L2} = \dfrac{1-D}{2D-1}\dfrac{v_o}{R}. \end{cases} \quad (5)$$

The output voltage gain and the inductor L_2 current gain can be defined, respectively, as

$$K_o = \frac{v_o}{v_i} = \frac{D}{2D-1} \times \left[\frac{1}{1 + \dfrac{r_s + (2D^2-2D+1)r_L + D(1-D)r_C}{(2D-1)^2R}} \right] \text{ and} \quad (6)$$

$$K_i = \frac{i_{L2}}{i_i} = \frac{1-D}{D}. \quad (7)$$

It should be noted that the output profile in (6) can be used for both resistive and inductive loading. The equations from (1) to (5) which lead to the output profile in (6) are unchanged when the load is inductive. Fig. 5 shows the output voltage gains versus the duty cycle D with a variable ratio of $k_r = (r_s + r_L)/R$ in the case of $r_L = r_C/2$. In the ideal case ($r_s = r_L = r_C = 0\,\Omega$) from (5), the following is obtained:

$$\begin{cases} v_o = \dfrac{D}{2D-1} v_i \\ v_{c2} = \dfrac{1-D}{2D-1} v_i \\ i_i = \dfrac{D}{2D-1}\dfrac{v_o}{R} \\ i_{L2} = \dfrac{1-D}{2D-1}\dfrac{v_o}{R}. \end{cases} \quad (8)$$

The output voltage gain has features that were reported in [1]–[3]. It is clear that there are two operation regions, as shown in Fig. 5. When the duty cycle is greater than 0.5, the output voltage is boosted and is in-phase with the input voltage. When the duty cycle is less than 0.5, the output voltage is bucked/boosted and out-of-phase with the input voltage.

Fig. 6 shows the relationship between the inductor L_2 current gain and the duty cycle. When the converter is operating in the boost in-phase mode ($D > 0.5$), the inductor L_2 current is bucked. When the converter is operating in the buck/boost out-of-phase mode ($D < 0.5$), the inductor L_2 current is boosted. The inductor L_2 current is in-phase with the input current.

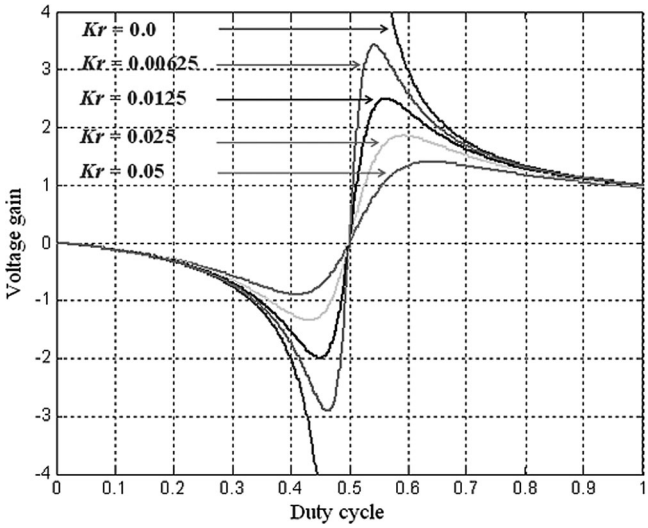

Fig. 5. Output voltage gain versus the duty cycle with the variable ratio of $k_r = (r_s + r_L)/R$.

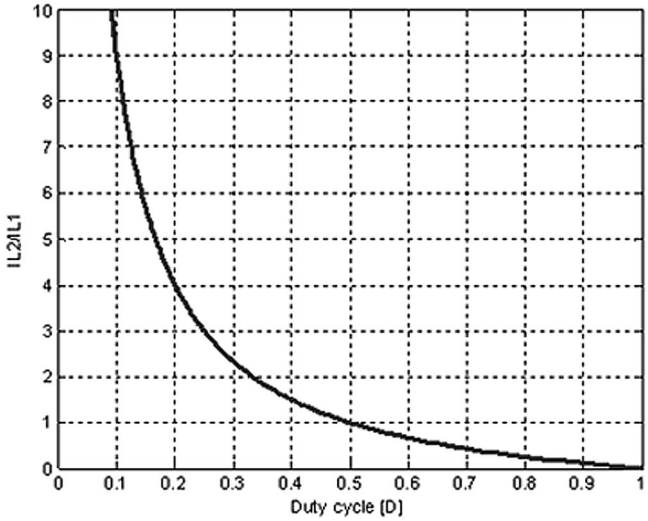

Fig. 6. Inductor L_2 current gain versus the duty cycle of the modified single-phase quasi-Z-source ac–ac converter.

Table II shows the voltage and current equations for the ideal case ($r_s = r_L = r_C = 0\ \Omega$) of the conventional single-phase Z-source ac–ac converters presented in [1] and [2] as well as for the single-phase quasi-Z-source ac–ac converters. In Table II, P_o is the output power and I_i, I_{L1}, I_{L2}, and V_i are the rms values of the input current, inductor L_1 current, inductor L_2 current, and the input voltage, respectively.

The quasi-Z-source network parameters are usually chosen according to the percentage of the current ripple through the inductor $x\%$, and to the percentage of the voltage ripple across the capacitor $y\%$ [2], [3]. Table III shows the parameter design of the conventional single-phase Z-source ac–ac converter [1], [2], the single-phase quasi-Z-source ac–ac converter [3], and the modified single-phase quasi-Z-source ac–ac converter. In Table III, $I_{\text{str, max}}$, $I_{S,\text{ rms}}$, and $V_{\text{CE, max}}$ are the peak current stress, the rms current stress, and the collector-emitter voltage

TABLE II
GOVERNING EQUATIONS OF THE CONVENTIONAL SINGLE-PHASE Z-SOURCE AC–AC CONVERTERS IN [1] AND [2] AND THE SINGLE-PHASE QUASI-Z-SOURCE AC–AC CONVERTERS IN THE IDEAL CASE ($r_s = r_L = r_C = 0\ \Omega$)

	Conventional converter [1], [2]	Quasi-Z-source converter [3]	Modified converter
$\frac{v_o}{v_i} = \frac{v_{C1}}{v_i}$	$\frac{D}{2D-1}$	$\frac{D}{2D-1}$	$\frac{D}{2D-1}$
$\frac{v_{C2}}{v_i}$	$\frac{D}{2D-1}$	$\frac{1-D}{2D-1}$	$\frac{1-D}{2D-1}$
$I_i = I_{LI}$	$\frac{P_o}{V_i}$	$\frac{P_o}{V_i}$	$\frac{P_o}{V_i}$
I_{L2}	$\frac{P_o}{V_i}$	$\frac{P_o}{V_i}$	$\frac{1-D}{D}\frac{P_o}{V_i}$

TABLE III
PARAMETER DESIGNS OF THE SINGLE-PHASE Z-SOURCE AC–AC CONVERTERS

	Conventional converter [1], [2]	Quasi-Z-source converter [3]	Modified quasi-Z-source converter
L	$L_1 = L_2 \geq \frac{\sqrt{2}D^2(1-D)TV_i^2}{(1-2D)^2 x\%P_o}$	$L_1 = L_2 \geq \frac{\sqrt{2}D(1-D)TV_i^2}{(1-2D)x\%P_o}$	$L_1 \geq \frac{\sqrt{2}D(1-D)TV_i^2}{(1-2D)x\%P_o}$ $L_2 \geq \frac{\sqrt{2}D^2TV_i^2}{(1-2D)x\%P_o}$
C	$C_1 = C_2 \geq \frac{\sqrt{2}(1-D)(2D-1)TP_o}{Dy\%V_i^2}$	$C_1 \geq \frac{\sqrt{2}(1-D)(2D-1)TP_o}{Dy\%V_i^2}$ $C_2 \geq \frac{\sqrt{2}(2D-1)TP_o}{y\%V_i^2}$	$C_1 \geq \frac{\sqrt{2}(1-D)(2D-1)TP_o}{Dy\%V_i^2}$ $C_2 \geq \frac{\sqrt{2}(2D-1)TP_o}{y\%V_i^2}$
$I_{str,\ max}$	$\frac{\sqrt{2}P_o}{DV_i}$	$\frac{\sqrt{2}P_o}{DV_i}$	$\frac{\sqrt{2}P_o}{DV_i}$
$I_{S,\ RMS}$	$I_{S1} = \frac{P_o}{\sqrt{D}V_i}$ $I_{S2} = \frac{\sqrt{1-D}P_o}{DV_i}$	$I_{S1} = \frac{P_o}{\sqrt{D}V_i}$ $I_{S2} = \frac{\sqrt{1-D}P_o}{DV_i}$	$I_{S1} = \frac{P_o}{\sqrt{D}V_i}$ $I_{S2} = \frac{\sqrt{1-D}P_o}{DV_i}$
$V_{CE,\ max}$	$\frac{\sqrt{2}}{2D-1}V_i$	$\frac{\sqrt{2}}{2D-1}V_i$	$\frac{\sqrt{2}}{2D-1}V_i$

stress of the switches S_{1j}, S_{2j} $(j = a, b)$, respectively. As shown in Tables II and III, the input current, the output voltage, the peak current stress, the rms current stress, and the collector-emitter voltage stress of switches S_{1j} and S_{2j} are the same for all of the converters. In Table III, we can see that the inductors and capacitors of each topology may be chosen using different values. Therefore, each converter has its optimized design in terms of loss reduction.

Different PWM strategies have been introduced in different applications. Depending on load conditions, some of these strategies have yields related to the input power factor (PF) while others focus on high efficiency. A modified sinusoidal PWM technique [32] is used to optimize the PF. Fig. 7 shows the PF control strategy block diagram. The input voltage v_i going through to the voltage detector shifted to the left by an angle α. The output phase-shift sinusoidal signal u_α that leads to v_i by an angle α is synthesized to a positive sinusoidal signal. This

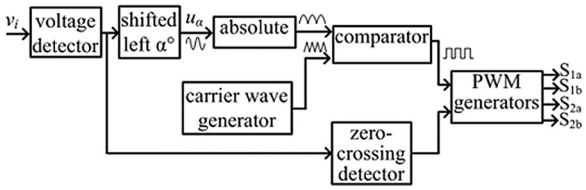

Fig. 7. Power factor control strategy block diagram.

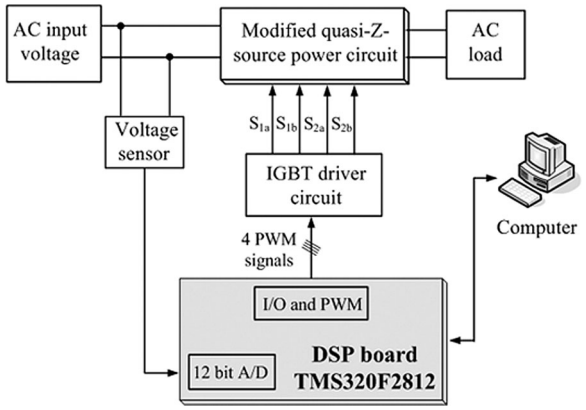

Fig. 8. Block diagram of the experimental system.

signal is compared with a triangle waveform to generate the switching pulses. On the other hand, the power factor is controlled via the phase-shift angle α, and this power factor control technique for ac chopper was described in detail in [32].

III. VERIFICATION EXPERIMENTS

In order to verify the properties described earlier, a laboratory prototype of the modified single-phase quasi-Z-source ac–ac converter was constructed. Fig. 8 shows a block diagram of the experimental system, which includes a microcontroller TMS320F2812 DSP, an IGBT driver circuit, and a modified single-phase quasi-Z-source ac–ac converter power circuit. The input voltage was produced by an ES2000S single-phase master (NF Corporation, Yokohama, Japan). An LEM LV25-P voltage transducer was connected across the input. The input voltage sensor signal was sent to the DSP via a 12-bit A/D converter. An unsigned long-type 12-bit (0–4095) signal from the A/D converter was compared to 2048 in order to detect the zero crossing point of the input voltage. Depending on the desired output voltage, the DSP generated four control PWM signals that controlled the four switches S_{1a}, S_{1b}, S_{2a}, and S_{2b}. The input power and the input power factor were measured by ES2000S whereas the output power was measured by a WT210 digital power meter (YOKOGAWA, Musashino, Japan). Four FAIRCHILD SGL60N90D insulated gate bipolar transistors (IGBTs) were used in building the hardware. The parameters used were $L_1 = L_2 = 1$ mH, $C_1 = C_2 = 6.8\ \mu$F, and $R = 30\ \Omega$. The switching frequency was set to 20 kHz and the dead time for commutation was set to 0.5 μs. The input voltage was 70 $V_{\rm rms}$/60 Hz.

Fig. 9 shows the experimental results based on a resistive load for the modified single-phase quasi-Z-source ac–ac converter when the input voltage is 70 $V_{\rm rms}$/60 Hz, $D = 0.75$, and

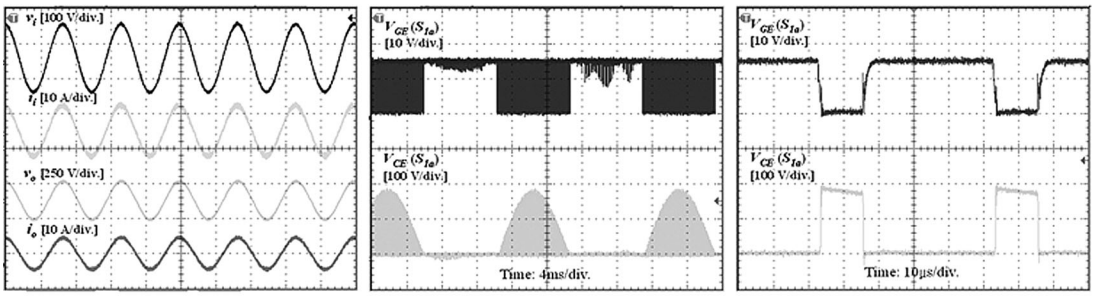

Fig. 9. Experimental results based on an *R* load for the boost in-phase mode when $D = 0.75$ and $V_i = 70\ \mathrm{V_{rms}}$. The measured $\mathrm{PF}_i = 0.991$, THD$i = 2.95\%$, and THDvo $= 1.96\%$. (a) From top to bottom: v_i (100 V/div); i_i (10 A/div); v_o (250 V/div); i_o (10 A/div). Time: 10 ms/div; (b) top: V_{GE} of S_{1a} (10 V/div); bottom: V_{CE} of S_{1a} (100 V/div). Time: 4 ms/div. (c) Top: V_{GE} of S_{1a} (10 V/div); bottom: V_{CE} of S_{1a} (100 V/div). Time: 10 μs/div.

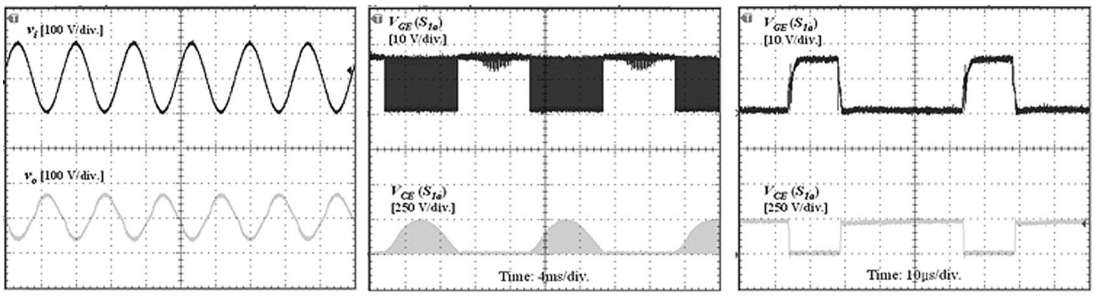

Fig. 10. Experimental results based on an *R* load for the buck out-of-phase mode when $D = 0.3$ and $V_i = 70\ \mathrm{V_{rms}}$. The measured $\mathrm{PF}_i = 0.975$. (a) Top: v_i (100 V/div); bottom: v_o (100 V/div). Time: 10 ms/div. (b) Top: V_{GE} of S_{1a} (10 V/div); bottom: V_{CE} of S_{1a} (100 V/div). Time: 4 ms/div. (c) Top: V_{GE} of S_{1a} (10 V/div); bottom: V_{CE} of S_{1a} (100 V/div). Time: 10 μs/div.

$R = 30\ \Omega$. In Fig. 9(a), the waveforms from top to bottom represent the input voltage, the input current, the output voltage, and the output current. When $D = 0.75$, the output voltage is boosted to 100 $\mathrm{V_{rms}}$ from the 70 $\mathrm{V_{rms}}$ input voltage and is in-phase with the input voltage. The measured input power factor PF_i is 0.991.

Fig. 10 shows the experimental results based on a resistive load for the modified single-phase quasi-Z-source ac–ac converter when the input voltage is 70 $\mathrm{V_{rms}}$/60 Hz, $D = 0.3$, and $R = 30\ \Omega$. In Fig. 10(a), the top waveform is the input voltage and the bottom waveform is the output voltage. When $D = 0.3$, the output voltage is bucked to 50 $\mathrm{V_{rms}}$ from the 70 $\mathrm{V_{rms}}$ input voltage and is out-of-phase with the input voltage. The PF_i is 0.975. In Figs. 9(b) and (c), and 10(b), and (c), the top waveform is the gate-emitter voltage of S_{1a} and the bottom waveform is the collector-emitter voltage of S_{1a}.

Fig. 11 shows the experimental results based on a passive *RL* load with $R = 30\ \Omega$ and $L = 30$ mH when $D = 0.75$ and $V_i = 70\ \mathrm{V_{rms}}$. The measured input power factor is 0.956. In Fig. 11(a), the waveforms from top to bottom are the input voltage, the output voltage, and the output current. In Fig. 11(b), the top waveform is the gate-emitter voltage of S_{1a} and the bottom waveform is the collector-emitter voltage of S_{1a}.

Fig. 12 shows the experimental results based on a nonlinear load when $D = 0.75$ and $V_i = 70\ \mathrm{V_{rms}}$. The nonlinear load consists of a single-phase diode-bridge rectifier and an *LC* output filter with $L = 3$ mH, $C = 470\ \mu$F, and $R = 30\ \Omega$. The measured input power factor is 0.839 and the THD of the

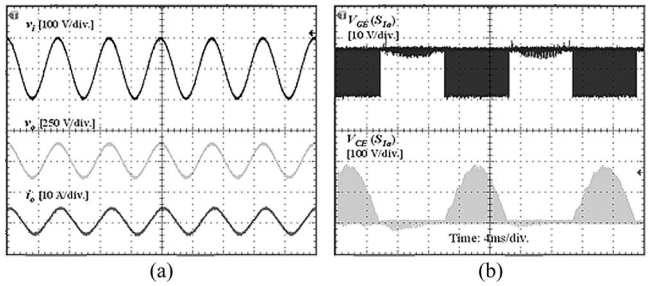

Fig. 11. Experimental results based on an *RL* load for the boost in-phase mode when $D = 0.75$, $V_i = 70\ \mathrm{V_{rms}}$. The measured $\mathrm{PF}_i = 0.956$. (a) Top: v_i (100 V/div); center: v_o (250 V/div); bottom: i_o (10 A/div). Time: 10 ms/div. (b) Top: V_{GE} of S_{1a} (10 V/div); bottom: V_{CE} of S_{1a} (100 V/div). time: 4 ms/div.

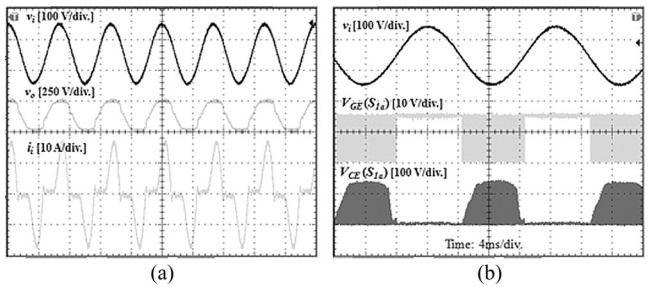

Fig. 12. Experimental results based on a nonlinear load for the boost in-phase mode when $D = 0.75$, $V_i = 70\ \mathrm{V_{rms}}$. The measured $\mathrm{PF}_i = 0.839$, THD$i = 55.98\%$. (a) Top: v_i (100 V/div); center: v_o (250 V/div); bottom: i_i (10 A/div). Time: 10 ms/div. (b) Top: v_i (100 V/div); center: V_{GE} of S_{1a} (10 V/div); bottom: V_{CE} of S_{1a} (100 V/div). Time: 4 ms/div.

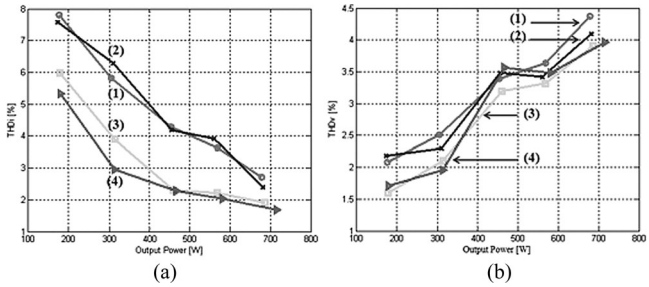

Fig. 13. Measured THD versus the output power based on a resistive load with $D = 0.75$. (a) THD of the input current (THD*i*). (b) THD of the output voltage (THDvo) [(1) original single-phase Z-source ac–ac converter [1], (2) conventional single-phase Z-source ac–ac converter [2], (3) single-phase quasi-Z-source ac–ac converter [3], and (4) modified single-phase quasi-Z-source ac–ac converter].

input current is 55.98%. In Fig. 12(a), the waveforms from top to bottom are the input voltage, the output voltage, and the input current. In Fig. 12(b), the top waveform is the input voltage, the center waveform is the gate-emitter voltage of S_{1a}, and the bottom waveform is the collector-emitter voltage of S_{1a}. As Figs. 9–12 show, there is no voltage spike on the switches. From these results, it can be seen that the use of the safe-commutation strategy provides a significant improvement in that it avoids voltage spikes on the switches.

Fig. 13 shows the measured THD of the input current and the output voltage of the converter topologies based on a resistive load *R* with a variable output power. The THD*i* of the input current of the modified single-phase quasi-Z-source ac–ac converter is less than 3% when the output power is more than 300 W. This THD*i* value is acceptable, even though an *LC* input filter is not attached to the modified single-phase quasi-Z-source ac–ac converter. The THDvo of the output voltage of the modified single-phase quasi-Z-source ac–ac converter is less than 4%. Fig. 14 shows the measured efficiency of the single-phase Z-source ac–ac converters from Fig. 1 with a variable output power. The experiment used to measure the THD and the efficiency of the conventional converters is implemented with the following conditions: 1) a small *RC* snubber circuit was added to S_1 and S_2 of the original single-phase Z-source ac–ac converter as shown in Fig. 1(a) [1]; 2) the parameters used for the *LC* input filter, as shown in Fig. 1(a) and (b), were $L_i = 0.1$ mH and $C_i = 10\ \mu$F; 3) the parameters used for the *LC* output filter, as shown in Fig. 1(a)–(c), were $L_f = 1.4$ mH and $C_f = 10\ \mu$F; and 4) the other parameters were kept constant in order to justify the efficiency comparison. As shown in Figs. 13 and 14, the modified single-phase quasi-Z-source ac–ac converter with the safe-commutation strategy has a lower THD and a higher efficiency when using the same values for the inductors and capacitors (and the same *LC* filters–just in case) for the four topologies studied.

Table IV shows the output ripple components of the proposed topology in comparison to the original quasi Z-source topology [3]. From Table IV, we can observe that the output ripple components of the modified single-phase quasi-Z-source ac–ac converter are higher than those of the single-phase quasi-Z-source ac–ac converter [3]. This can be explained as follows.

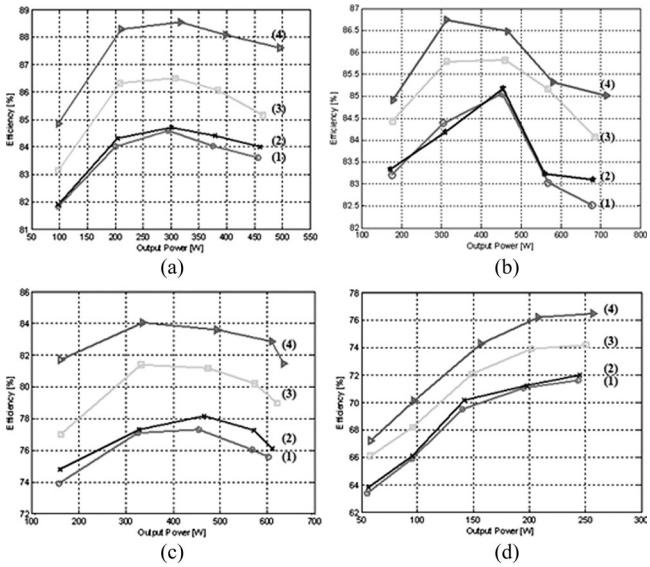

Fig. 14. Measured efficiency versus the output power with different duty cycles [(1) the original single-phase Z-source ac–ac converter [1], (2) the conventional single-phase Z-source ac–ac converter [2], (3) the single-phase quasi-Z-source ac–ac converter [3], and (4) the modified single-phase quasi-Z-source ac–ac converter].

TABLE IV
OUTPUT RIPPLE COMPONENTS OF THE PROPOSED TOPOLOGY COMPARED TO ORIGINAL QUASI Z-SOURCE TOPOLOGY

	Quasi-Z-source converter [3]	Modified converter
$I_o\%$	2.84%	4.42%
$V_o\%$	2.71%	4.31%

Tables I and II show the voltage ripple across the capacitors of both converters is the same when the quasi-Z-network parameters are the same. The output voltage of the proposed topology equals the voltage across the capacitor C_1 as shown in Fig. 1(d). Besides, the output voltage of the original topology is the voltage across the capacitor C_f of the second order *LC* output filter as shown in Fig. 1(c). Therefore, the output ripple components of the single-phase quasi-Z-source ac–ac converter reduce compared to those of the modified single-phase quasi-Z-source ac–ac converter. In the table, $I_o\%$ and $V_o\%$ are the ratio of the peak-peak output ripple current with respect to the peak value of the output current and the ratio of the peak-peak output ripple voltage with respect to the peak value of the output voltage, respectively.

From the experimental results, it can be seen that the modified single-phase quasi-Z-source ac–ac converter inherits all of the advantages of the conventional converters in which the output is bucked/boosted and in-phase or out-of-phase with the input voltage. In addition, the modified single-phase quasi-Z-source ac–ac converter has the unique advantages of a smaller size, a lower THD*i*, a higher input power factor, and a higher efficiency in comparison to the conventional converters.

IV. Conclusion

A single-phase Z-source converter for ac–ac power conversion has been presented in this paper. The proposed converter, called a modified single-phase quasi-Z-source ac–ac converter, inherits all of the advantages of a traditional single-phase Z-source ac–ac converter; it can perform buck–boost output voltages, as well as maintaining or reversing the phase angle all the while sharing the same ground. In addition, the modified single-phase quasi-Z-source ac–ac converter has the unique advantages in that the size of the converter is reduced and the operation of the input current is continuous, with additional features, such as a reduction in the in-rush, a harmonic current, and an improved power factor. A safe-commutation strategy is applied to the modified single-phase quasi-Z-source ac–ac converter. The use of this safe-commutation strategy is a significant improvement, as it makes it possible to avoid voltage spikes on the switches without the use of a snubber circuit. The operating principles and a steady-state analysis are presented.

Experimental results show that the modified single-phase quasi-Z-source ac–ac converter has a higher efficiency in comparison to the conventional single-phase Z-source ac–ac converters, and that there is no voltage spike on the switch. With the use of duty-ratio control, the converter is essentially a "solid-state transformer" with a continuously variable turn ratio. The converter can be used to compensate for voltage sags and swells in ac–ac line conditioning.

References

[1] X. P. Fang, Z. M. Qian, and F. Z. Peng, "Single-phase Z-source PWM ac–ac converters," *IEEE Power Electron. Lett.*, vol. 3, no. 4, pp. 121–124, Dec. 2005.

[2] Y. Tang, S. Xie, and C. Zhang, "Z-source ac–ac converters solving commutation problem," *IEEE Trans. Power Electron.*, vol. 22, no. 6, pp. 2146–2154, Nov. 2007.

[3] M. K. Nguyen, Y. G. Jung, and Y. C. Lim, "Single-phase ac–ac converter based on quasi-Z-source topology," *IEEE Trans. Power Electron.*, vol. 25, no. 8, pp. 2200–2210, Aug. 2010.

[4] F. Z. Peng, L. Chen, and F. Zhang, "Simple topologies of PWM ac–ac converters," *IEEE Power Electron. Lett.*, vol. 1, no. 1, pp. 10–13, Mar. 2003.

[5] F. L. Luo and H. Ye, "Research on dc-modulated power factor correction ac/ac converters," in *Proc. IEEE Industrial Electronics Conf.*, 2007, pp. 1478–1483.

[6] N. A. Ahmed, K. Amei, and M. Sakui, "A new configuration of single-phase symmetrical PWM ac chopper voltage controller," *IEEE Trans. Ind. Electron.*, vol. 46, no. 5, pp. 942–952, Oct. 1999.

[7] R. Stala, S. Pirog, A. Mondzik, M. Baszynski, A. Penczek, J. Czekonski, and S. Gasiorek, "Results of investigation of multicell converters with balancing circuit. Part II," *IEEE Trans. Ind. Electron.*, vol. 56, no. 7, pp. 2620–2628, Jul. 2009.

[8] R. H. Wilkinson, T. A. Meynard, and H. T. Mouton, "Natural balance of multicell converters: The general case," *IEEE Trans. Power Electron.*, vol. 21, no. 6, pp. 1658–1666, Nov. 2006.

[9] L. Li, J. Yang, and Q. Zhong, "Novel family of single-stage three-level ac choppers," *IEEE Trans. Power Electron.*, vol. 26, no. 2, pp. 504–511, Feb. 2011.

[10] D. Chen and J. Liu, "The uni-polarity phase-shifted controlled voltage mode ac–ac converters with high frequency AC link," *IEEE Trans. Power Electron.*, vol. 21, no. 4, pp. 899–905, Jul. 2006.

[11] S. Subramanian and M. K. Mishra, "Interphase ac–ac topology for voltage sag supporter," *IEEE Trans. Power Electron.*, vol. 25, no. 2, pp. 514–518, Feb. 2009.

[12] D. M. Lee, T. G. Habetler, R. G. Harley, T. L. Keister, and J. R. Rostron, "A voltage sag supporter utilizing a PWM-switched autotransformer," *IEEE Trans. Power Electron.*, vol. 22, no. 2, pp. 626–635, Mar. 2007.

[13] D. M. Divan and J. Sastry, "Voltage synthesis using dual virtual quadrature sources—A new concept in ac power conversion," *IEEE Trans. Power Electron.*, vol. 23, no. 6, pp. 3004–3013, Nov. 2008.

[14] Z. Ye, "Three-phase reactive power compensation using a single-phase ac/ac converter," *IEEE Trans. Power Electron*, vol. 14, no. 5, pp. 816–822, Sep. 1999.

[15] M. K. Nguyen, Y. G. Jung, Y. C. Lim, and Y. M. Kim, "A single-phase Z-source buck-boost matrix converter," *IEEE Trans. Power Electron.*, vol. 25, no. 2, pp. 453–462, Feb. 2010.

[16] M. K. Nguyen, Y. G. Jung, and Y. C. Lim, "Single-phase Z-source ac–ac converter with wide range output voltage operation," *J. Power Electron.*, vol. 9, no. 5, pp. 736–747, Sep. 2009.

[17] J. H. Youm and B. H. Kwon, "Switching technique for current-controlled ac-to-ac converters," *IEEE Trans. Ind. Electron.*, vol. 46, no. 2, pp. 309–318, Apr. 1999.

[18] M. K. Nguyen, Y. G. Jung, H. Y. Yang, and Y. C. Lim, "Single-phase Z-source cycloconverter with safe-commutation strategy," *IET Power Electron.*, vol. 3, no. 2, pp. 232–242, Mar. 2010.

[19] F. Z. Peng, "Z-source inverter," *IEEE Trans. Ind. Appl.*, vol. 39, no. 2, pp. 504–510, Mar./Apr. 2003.

[20] P. C. Loh, F. Blaabjerg, and C. P. Wong, "Comparative evaluation of pulse width modulation strategies for Z-source neutral-point-clamped inverter," *IEEE Trans. Power Electron.*, vol. 22, no. 3, pp. 1005–1013, May 2007.

[21] F. Z. Peng, M. Shen, and K. Holland, "Application of Z-source inverter for traction drive of fuel cell-battery hybrid electric vehicles," *IEEE Trans. Power Electron.*, vol. 22, no. 3, pp. 1054–1061, May 2007.

[22] M. Zhu, K. Yu, and F. L. Luo, "Switched-inductor Z-source inverter," *IEEE Trans. Power Electron.*, vol. 25, no. 8, pp. 2150–2158, Aug. 2010.

[23] C. J. Gajanayake, F. L. Luo, H. B. Gooi, P. L. So, and L. K. Siow, "Extended boost Z-source inverters," *IEEE Trans. Power Electron.*, vol. 25, no. 10, pp. 2642–2652, Oct. 2010.

[24] J. Anderson and F. Z. Peng, "Four quasi-Z-source inverters," in *Proc. IEEE Power Electronics Specialists Conf.*, 2008, pp. 2743–2749.

[25] Y. Tang, S. Xie, C. Zhang, and Z. Xu, "Improved Z-source inverter with reduced Z-source capacitor voltage stress and soft-start capability," *IEEE Trans. Power Electron.*, vol. 24, no. 2, pp. 409–415, Feb. 2009.

[26] S. M. Dehnavi, M. Mohamadian, A. Yazdian, and F. Ashrafzadeh, "Space vectors modulation for nine-switch converters," *IEEE Trans. Power Electron.*, vol. 25, no. 6, pp. 1488–1496, Jun. 2010.

[27] S. M. Dehghan, M. Mohamadian, A. Yazdian, and F. Ashrafzadeh, "A dual-input–dual-output Z-source inverter," *IEEE Trans. Power Electron.*, vol. 25, no. 2, pp. 360–368, Feb. 2010.

[28] P. C. Loh, F. Gao, F. Blaabjerg, and S. W. Lim, "Operational analysis and modulation control of three-level Z-source inverters with enhanced output waveform quality," *IEEE Trans. Power Electron.*, vol. 24, no. 7, pp. 1767–1775, Jul. 2009.

[29] P. C. Loh, F. Gao, P. C. Tan, and F. Blaabjerg, "Three-level ac–dc–ac Z-source converter using reduced passive component count," *IEEE Trans. Power Electron.*, vol. 24, no. 7, pp. 1671–1681, Jul. 2009.

[30] H. Cha, F. Z. Peng, and D. W. Yoo, "Distributed impedance network (Z-network) dc–dc converter," *IEEE Trans. Power Electron.*, vol. 25, no. 11, pp. 2722–2733, Nov. 2010.

[31] X. Fang and F. Z. Peng, "Novel three-phase current-fed Z-source ac–ac converter," *Conf. Rec. of IEEE Power Electronics Specialists Conf.*, 2007. pp. 2993–2996.

[32] K. Geargakas and A. Safacas, "Modified sinusoidal pulse-width modulation operation technique of an ac–ac single-phase converter to optimise the power factor," *IET Power Electron.*, vol. 3, no. 3, pp. 454–464, 2010.

Minh-Khai Nguyen (S'09) was born in Vietnam in 1982. He received the B.S. degree in electrical and electronics engineering from the Ho Chi Minh University of Technology, Ho Chi Minh city, Vietnam, in 2005, and the M.S. and Ph.D. degrees in electrical engineering from Chonnam National University, Gwangju, Korea, in 2007 and 2010, respectively.

Since 2010, he has been a Lecturer with Nguyen Tat Thanh University, Ho Chi Minh city, Vietnam. In 2011, he was a Visiting Researcher with the Biohousing Research Institute, Chonnam National University, Korea. His current research interests include switched reluctance motor drives, power quality, and Z-source converters.

Young-Cheol Lim (M'85) was born in Chonnam, Korea, in 1953. He received the B.S. degree in electrical engineering from Chonnam National University, Gwangju, Korea, in 1975, and the M.S. and Ph.D. degrees from the Korea University, Seoul, Korea, in 1977 and 1990, respectively.

Since 1981, he has been a Professor with Chonnam National University, where he was the Director of the Research Center for High-Quality Electric Components and Systems from 1998 to 2007. He is the coauthor of three books. He has authored or coauthored more than 200 published technical papers. His current research interests include power electronics, control instruments, and neurofuzzy control.

Dr. Lim was the President of Korea Institute of Power Electronics (KIPE) in 2009. He has been engaged with various academic societies, such as the KIPE, the Korean Institute of Electrical Engineers, and the Institute of Control, Automation, and Systems Engineers, Korea. He received a number of awards, including 2000 KIPE Best Paper Award and 2001 KIPE Academic Award.

Yong-Jae Kim (S'04–M'07) was born in Gwnagju, Korea, in 1973. He received the B.Eng. degree in electrical engineering from Chosun University, Gwangju, Korea, in 1996 and the M.Eng. and Dr.Eng. degrees in electrical and electronic engineering from Musashi Institute of Technology, Tokyo, Japan, in 2003 and 2006, respectively.

He was a Researcher of Electrical and Electronic Engineering at Musashi Institute of Technology, Tokyo, Japan, from 2006 to 2007. He is currently an Associate Professor with the Department of Electrical Engineering, Chosun University, Gwnagju, Korea. His current research interests include the design and the numerical analysis of electric machines and ac servo drive systems.